Electromagnetically induced grating via enhanced nonlinear modulation by spontaneously generated coherence

Ren-Gang Wan, Jun Kou, Li Jiang, Yun Jiang, and Jin-Yue Gao

Phys. Rev. A **83**, 033824 — Published 23 March 2011

DOI: 10.1103/PhysRevA.83.033824

Electromagnetically induced grating via enhanced nonlinear modulation by spontaneously generated coherence

Ren-Gang Wan, Jun Kou, Li Jiang, Yun Jiang, and Jin-Yue Gao*

Key Lab of Coherent Light and Atomic and Molecular Spectroscopy of Ministry of Education, College of Physics, Jilin University, Changchun 130023, China

Corresponding author: jygao@mail.jlu.edu.cn

By investigating the third order nonlinearity of a four-level ladder-type atomic system, it is found that, with spontaneously generated coherence (SGC) present, the nonlinear absorption or refraction can be significantly enhanced with vanishing linear absorption. We attribute the enhancement of nonlinearity mainly to quantum interference in the two decay pathways from the two upper closely lying levels. With a standing-wave trigger field, absorption or phase grating, which effectively diffracts a weak probe into high-order direction, can be induced by the SGC enhanced absorptive or refractive nonlinear modulation. In contrast to the schemes for enhancing nonlinearity, no additional coupling field is required. Moreover, the present gratings result from the nonlinear modulation which differs from the recent investigations based on linear modulation.

PACS number(s): 42.50.Gy, 42.65.-k, 42.65.An

I. INTRODUCTION

Nonlinear optical phenomenon is well known as a fundamental process resulting from the interaction between light and matter. Especially the third order nonlinearity plays an important role and has many applications in polarization phase gates [1-3], optical switch [4,5], the generation of optical solitons [6,7], etc. However, the absence of sufficient nonlinearity and large

absorption in conventional media become obstacles to its applications, therefore, giant third order nonlinearity at low light level is desirable in various optical devices. To avoid these disadvantages, coherently driven multilevel electromagnetically induced transparency (EIT) systems were proposed to enhance third order Kerr nonlinearity with vanishing linear absorption and then large self- or cross- phase modulation (SPM or XPM) can be achieved [8-13]. Recently, giant Kerr nonlinearity was also obtained in active Raman gain (ARG) media [14].

The above studies on the enhancement of nonlinearity are all based on the laser induced atomic coherence in multilevel atoms, and it is crucial to have at least one coupling laser to create the necessary coherence. However, the atomic coherence can also occur in the process of spontaneous emission, in which the atom decays from closely placed upper levels to a single ground level. The quantum interference between the decay channels, which is called spontaneously generated coherence (SGC), can lead to many phenomena, such as amplification without inversion [15,16], narrowing and quenching of spontaneous emission [17-23], refractive index enhancement without absorption [24], and giant SPM [25]. Another novel phenomenon caused by SGC is that it can induce dark state for a light-matter system and make a medium transparent to a short laser pulse [26,27]. In contrast to the lossless propagation in three level EIT media, no coupling laser field is required.

In this paper, we investigate the effect of SGC on the third order cross nonlinear interaction between the probe field and the trigger field in a four-level ladder-type system. When the trigger is resonant, the nonlinear two-photon absorption can be enhanced by constructive quantum interference, while the linear absorption is vanishing due to the destructive quantum interference between the two decay channels. We can also obtain enhanced nonlinear refraction with both linear and nonlinear absorption neglectable in the case of a large detuned trigger field. The

enhancement of nonlinearity in this system is a result of inherent quantum interference in the decay so that no coupling laser fields are required for transparency. We then exploit the enhanced nonlinearity to a type of all optical device. By using a trigger with standing-wave intensity pattern, the probe experiences a periodic variation of absorption or refractive index, and therefore, the medium acts an absorption or phase grating and can effectively diffract the probe into high order directions. This phenomenon is called electromagnetically induced grating (EIG), which is usually studied in EIT-based systems [28-30]. However, the gratings here are created by the nonlinear modulation which is different from the recent EIG schemes based on linear modulation. Moreover, the nonlinear modulation can lead to almost pure phase grating with high diffraction efficiency which cannot be obtained in the hybrid grating by linear modulation. We would like to point out that nonlinear modulation was proposed to achieve phase grating [31], however it is based on EIT and a coupling field is required.

Note, however, that SGC only exists in such atoms having closely lying upper levels and that corresponding dipole matrix elements are nor orthogonal. That is, the upper levels should have the same J and m_J quantum numbers [32]. But the rigorous conditions of near-degenerated levels and nonorthogonal dipole moments are rarely met in real atoms so no experiment has been carried out in atoms to observe the SGC effect directly. However, such type quantum interference results from the incoherent decay processes can be realized in many other systems. Examples include spontaneous emission in dimer [29], autoionizing resonances [34, 35], tunneling effect in quantum wells [36-38]. Modified vacuum, such as cavity field or anisotropy vacuum, can even lead to quantum interference among the decay channels with orthogonal dipole moments [39-41]. The SGC effect can be also simulated with atoms in the dressed-state picture [42-45]. Therefore, although our proposed scheme is difficultly carried out with atom in

free vacuum, it can be equally applied and achieved with the above systems.

This paper is organized as follows: In Sec. II the effect of SGC on the third order nonlinear susceptibility is investigated, and it is found that SGC can enhance the nonlinearity while keeping the linear absorption vanished. In Sec. III, by using a standing-wave trigger field, we exploit the enhanced nonlinear modulation to obtain pure absorption and phase gratings which can effectively diffract the weak probe to high order directions. Finally we present conclusions in Sec. IV.

II. ENHANCED THIRD ORDER NONLINEARITY VIA SGC

We consider a four-level double-ladder atomic system shown in Fig. 1(a). A weak probe field couples the ground state $|1\rangle$ to two closely lying upper states $|2\rangle$ and $|3\rangle$ with Rabi frequencies $\Omega_{p1}=\vec{E}_p\cdot\vec{d}_{12}/2\hbar$ and $\Omega_{p2}=\vec{E}_p\cdot\vec{d}_{13}/2\hbar$. The states $|2\rangle$ and $|3\rangle$ are simultaneously coupled to the excited state $|4\rangle$ by a trigger field. The corresponding Rabi frequencies are $\Omega_{T1}=\vec{E}_T\cdot\vec{d}_{24}/2\hbar$ and $\Omega_{T2}=\vec{E}_T\cdot\vec{d}_{34}/2\hbar$. E_p (E_T) represents the amplitude of the probe (trigger) field and $\vec{d}_{ij}$ denotes the electric-dipole moment of transition $|i\rangle\leftrightarrow|j\rangle$. For simplicity, we assume in the following that $d_{13}/d_{12}=p$ ($d_{34}/d_{24}=q$) and the misalignment angle α between $\vec{d}_{13}$ and $\vec{d}_{12}$ is equally partitioned by $\vec{E}_p$ while $\vec{d}_{34}$ is parallel (antiparallel) to $\vec{d}_{24}$, as shown in Fig. 1(b). Then we have $\Omega_{p1}=\Omega_{p2}/p=\Omega_p$ and $\Omega_{T1}=\Omega_{T2}/q=\Omega_T$.

Under the electric-dipole and rotating-wave approximation, utilizing the Weisskopf-Wigner theory of spontaneous emission, the system dynamics can be described by equations of motion for the probability amplitudes of the states given as:

$$\dot{a}_1 = i\Omega_p a_2 + ip\Omega_p a_3, \tag{1a}$$

$$\dot{a}_2 = i(\Delta_p - \delta)a_2 + i\Omega_p a_1 + i\Omega_T a_4 - \frac{\Gamma_2}{2}a_2 - \frac{\eta\sqrt{\Gamma_2\Gamma_3}}{2}a_3, \tag{1b}$$

$$\dot{a}_3 = i(\Delta_p + \delta)a_3 + ip\Omega_p a_1 + iq\Omega_T a_4 - \frac{\Gamma_3}{2}a_3 - \frac{\eta\sqrt{\Gamma_2\Gamma_3}}{2}a_2, \tag{1c}$$

$$\dot{a}_4 = i(\Delta_p + \Delta_T)a_4 + i\Omega_T a_2 + iq\Omega_T a_3 - \frac{\Gamma_4}{2}a_4, \tag{1d}$$

where Γ_2, Γ_3 and Γ_4 are the spontaneous decay rates from the corresponding states. $\Delta_p = \omega_p - (\omega_{21} + \omega_{31})/2$ and $\Delta_T = \omega_T - (\omega_{42} + \omega_{43})/2$ denote the detuning of the probe and trigger fields, respectively. The frequency difference of the two closely lying state $|2\rangle$ and $|3\rangle$ is 2δ. The cross coupling term between the two spontaneous emission pathways, which refers to the quantum interference effect or SGC, is described as $\eta\sqrt{\Gamma_2\Gamma_3}/2$, where $\eta = \vec{d}_{12}\cdot\vec{d}_{13}/\left|\vec{d}_{12}\right|\left|\vec{d}_{13}\right| = \cos\alpha$ denotes the alignment of the two spontaneous emission dipole matrix elements. If these dipole matrix elements are parallel, i.e. $\alpha = 0$ and $\eta = 1$, the system exhibits quantum interference generated from the two spontaneous emission pathways, while if $\alpha = \pi/2$ and $\eta = 0$, there is no SGC. Such a system can be also achieved in Rb dimer, autoionizing system, quantum wells, cavity or anisotropy vacuum coupled atomic systems, and atomic system in dressed-state picture.

In the steady state, we solve the coupled amplitude equations under the weak field approximation ($|a_1|^2 = 1$). Then from the polarization of the medium, i.e. $P_p = \varepsilon_0\chi_p E_p = 2N(d_{12}a_2a_1^* + d_{13}a_3a_1^*)$, we can obtain the probe susceptibility χ_p given by

$$\chi_p = -\frac{Nd_{12}^2}{\varepsilon_0 \hbar} \cdot \chi, \tag{2a}$$

where N is the atomic density, and χ can be written as

$$\chi = \frac{\gamma_4'(p^2\gamma_2' + \gamma_3' - 2ip\gamma_{23}) - (p-q)^2\Omega_T^2}{\gamma_4'(\gamma_2'\gamma_3' + \gamma_{23}^2) - \Omega_T^2(q^2\gamma_2' + \gamma_3' - 2iq\gamma_{23})}, \tag{2b}$$

where $\gamma_2' = \Delta_p - \delta + i\Gamma_2/2$, $\gamma_3' = \Delta_p + \delta + i\Gamma_3/2$ and $\gamma_{23} = \eta\sqrt{\Gamma_2\Gamma_3}/2$. What we are interested in is the cross Kerr nonlinearity between the trigger and probe fields. Then we expand the probe susceptibility χ_p into the second order of Ω_T which can be written as

$$\chi_p = \frac{Nd_{12}^2}{\varepsilon_0 \hbar} \cdot [\chi^{(1)} + \chi^{(3)}\Omega_T^2], \tag{3a}$$

where $\chi^{(1)}$ and $\chi^{(3)}$ correspond to the first order linear and third order cross Kerr nonlinear parts of the probe susceptibility, respectively, which are given by

$$\chi^{(1)} = -\frac{p^2\gamma_2' + \gamma_3' - 2ip\gamma_{23}}{\gamma_2'\gamma_3' + \gamma_{23}^2}, \tag{3b}$$

$$\chi^{(3)} = \frac{1}{\gamma_4'(\gamma_2'\gamma_3' + \gamma_{23}^2)} \cdot [(p-q)^2 - \frac{(p^2\gamma_2' + \gamma_3' - 2ip\gamma_{23})(q^2\gamma_2' + \gamma_3' - 2iq\gamma_{23})}{\gamma_2'\gamma_3' + \gamma_{23}^2}]. \tag{3c}$$

From Eq. (3b) one finds that the linear probe susceptibility vanishes at the frequency:

$$\Delta_p = \frac{p^2 - 1}{p^2 + 1} \cdot \delta, \tag{4a}$$

when

$$\eta = 1, \quad p^2\Gamma_2 = \Gamma_3. \tag{4b}$$

In such a case, the medium is transparent to the probe field and no spontaneous emission occurs as a result of destructive quantum interference. In the steady state, the system evolves into dark state with all the population trapping in the state

$$|\psi_{Dark}\rangle = \mathcal{N}\left(\frac{2\delta\sqrt{\Gamma_2\Gamma_3}}{\Gamma_2+\Gamma_3}|1\rangle + \Omega_{p2}|2\rangle - \Omega_{p1}|3\rangle\right), \tag{5}$$

where $\mathcal{N}$ is the normalization factor.

While in the presence of the trigger field, it couples the dark state to the state $|4\rangle$ which leads to two-photon absorption. With a resonant trigger field, the corresponding two-photon transition probability is $P_{Dark\to 4} \propto \left|\Omega_{p2}\Omega_{T1} - \Omega_{p1}\Omega_{T2}\right|^2$, which can be written as $P_{Dark\to 4} \propto \Omega_p\Omega_T \cdot (p-q)^2$. If $p = q$, the transition probability is zero, then the dark state keeps unperturbed and the probe field experiences no absorption due to destructive quantum interference in the two-photon transition. Hence there is no nonlinear interaction at the transparency position determined by Eq. 4(a). However, when $pq < 0$, both the probe and trigger fields are absorbed via two-photon absorption as a result of constructive quantum interference. The same results can also be derived from Eq. (3c). When the probe field is at the transparent frequency, the second term in Eq. (3c) disappears, and remain only the first term which is proportional to $(p-q)^2$. Therefore, we can obtain enhanced nonlinearity for the probe field by setting $pq < 0$ even though the linear probe absorption is vanishing. In the following discussions, we assume that $p = 1$ and $q = -1$, then $\Gamma_2 = \Gamma_3$ according to Eq. (4b).

We now focus on the effect of SGC on the probe susceptibility through numerical simulation. For simplicity, we set $\Gamma_2 = \Gamma_3 = \gamma$ and all the other parameters are scaled by γ. Figure 2(a) and 2(b) show the absorptive ($\mathrm{Im}[\chi^{(1)}]$) and refractive ($\mathrm{Re}[\chi^{(1)}]$) parts of the linear susceptibility as a function of the probe detuning with SGC (black solid line) and without SGC (red dashed line), respectively. In the absence of SGC ($\eta = 0$), the probe is absorbed and the corresponding absorptive spectrum is the incoherent sum of two Lorentzian functions. However,

in the presence of SGC, the destructive quantum interference between the spontaneous emission from the two upper states makes the medium transparent to the probe field at particular frequency ($\Delta_p = 0$), and what's more, the dispersion becomes strong and steep due to SGC. Figure 2(c) and 2(d) display the absorptive ($\mathrm{Im}[\chi^{(3)}]$) and refractive ($\mathrm{Re}[\chi^{(3)}]$) parts of the third order nonlinearity with resonant trigger field ($\Delta_T = 0$). As can be seen, both the nonlinear absorption and the nonlinear refraction are enhanced via SGC. At the transparent position of $\Delta_p = 0$, the atom-field system is in the dark state in the presence of SGC, hence there are more population trapped in the two closely lying upper states $|2\rangle$ and $|3\rangle$. As a result, the two-photon absorption is enhanced as shown in Fig. 2(c). However, $\mathrm{Re}[\chi^{(3)}] = 0$ at $\Delta_p = 0$ and large nonlinear refractive index at $\Delta_p \neq 0$ is accompanied by significant linear and nonliear absorption. To obtain large Kerr nonlinearity with vanishing linear and nonlinear absorption, an off resonant trigger field is required. As shown in Fig. 2(e) and 2(f), the cross Kerr nonlinearity is enhanced accompanied by neglectable two-photon absorption with $\Delta_T = -25$ via SGC.

III. SGC-ASSISTED ELECTROMAGNETICALLY INDUCED GRATING

The enhanced two-photon absorption and Kerr nonlinearity have many applications in all optical switching, polarization phase gate. In the following, we propose a new type of all optical device utilizing the SGC-assisted large third order nonlinearity.

Due to the intensity dependent third order nonlinear absorption and refractive index, a trigger field with intensity pattern can produce absorption and phase pattern for the probe field. Therefore, when the trigger has a standing-wave pattern, the probe field experiences a periodic variation of the absorption or refractive index. Therefore, the probe, which propagates perpendicularly to the standing-wave, can be diffracted by the electromagnetically induced

grating.

The schematic diagram of the EIG is shown in Fig. 3. Two counter-propagating components of the trigger fields form a standing-wave along the x-direction, and then lead to intensity dependent atom-field interaction. The probe passes through the standing-wave region in the z-direction and acquires periodical absorption and phase modulation. Therefore, an absorption or phase diffraction grating is formed.

In order to obtain the diffraction pattern for the probe field propagating through the medium, we begin with the Maxwell's equation. Under the slowly varying amplitude approximation and in the steady-state regime, the self-consistent equation for E_p is given by

$$\frac{\partial E_p}{\partial z} = i\frac{\pi}{\varepsilon_0 \lambda_p} P_p, \tag{6a}$$

where λ_p is the wavelength of probe field. Equation (6a) can be rewritten as

$$\frac{\partial E_p}{\partial z'} = i\chi\gamma E_p, \tag{6b}$$

where $z' = (\pi N d_{12}^2)/(\hbar\varepsilon_0\lambda_p\,\gamma)\cdot z$. z' can be made dimensionless by setting $z_0 = (\hbar\varepsilon_0\lambda_p\gamma)/(\pi N d_{12}^2)$ as the unit for z. When taking only the first and third order susceptibilities into account, we have

$$\frac{\partial E_p}{\partial z'} = i(\chi^{(1)} + \chi^{(3)}\Omega_T^2)\gamma E_p, \tag{6c}$$

Then the complex transmission function for an interaction length L of the medium can be derived from Eqs. (6b) and (6c) as

$$T = \mathrm{e}^{-\mathrm{Im}[\chi]\gamma L}\mathrm{e}^{i\,\mathrm{Re}[\chi]\gamma L}, \tag{7a}$$

$$T = \mathrm{e}^{-\mathrm{Im}[\chi^{(1)}+\chi^{(3)}\Omega_T^2]\gamma L}\mathrm{e}^{i\,\mathrm{Re}[\chi^{(1)}+\chi^{(3)}\Omega_T^2]\gamma L}, \tag{7b}$$

where the first and second terms in the exponential correspond respectively to the absorption and phase modulation. For a standing-wave trigger field with Rabi frequency $\Omega_T(x) = \Omega_{T0}\sin(\pi x/\Lambda)$, where Λ is the spatial frequency of the standing-wave, the transmission function is modulated in the x-direction as gratings. Then by Fourier transformation of T, we obtain the Fraunhofer diffraction equation given by

$$I_p(\theta) = |F(\theta)|^2 \frac{\sin^2(M\pi\Lambda\sin\theta/\lambda_p)}{M^2\sin^2(\pi\Lambda\sin\theta/\lambda_p)}, \tag{8a}$$

where

$$F(\theta) = \int_0^{\Lambda} T\exp(-i2\pi x\sin\theta/\lambda_p)dx \tag{8b}$$

represents the Fraunhofer diffraction of a single space period, M is the number of spatial periods of the grating, and θ is the diffraction angle with respect to the z-direction. The nth order diffraction angle is determined by the grating equation, $\sin\theta = n\lambda_p/\Lambda$. Therefore, we can obtain the first order diffraction intensity as

$$I_p(\theta_1) = |F(\theta_1)|^2 = \left|\int_0^{\Lambda} T\exp(-i2\pi x/\Lambda)dx\right|^2, \tag{9}$$

A. Absorption grating

As pointed out in the above discussions, when the trigger field is resonant, the probability of two-photon absorption is maximal accompanied by vanishing linear absorption and no refraction. Hence, the trigger field with standing-wave intensity pattern can lead to periodic absorption modulation across the beam profile of the probe field and no phase modulation takes place. Figure 4(a) and (4b) show respectively the amplitude ($|T(x)|$) and phase (Φ) of the transmission function T. In the absence of SGC, the medium is opaque to the probe and the absorption modulation depth is small [red dashed line in Fig. (4a)], which restrict the diffraction efficiency

[red dashed line in Fig. (4d)]. However, when SGC effect is present, the destruction quantum interference leads to transparency for the probe field at the nodes of standing-wave, and the construction quantum interference results in two-photon absorption at the antinodes. As a result, the average transmissivity is higher and the absorption modulation depth is larger than in the case of no SGC [black solid line in Fig. (4a)]. Therefore, the diffraction efficiency can be enhanced with the assistance of SGC [black solid line in Fig. (4c)].

The role of SGC is twofold in the enhancement of diffraction efficiency for the EIG. One is that SGC induces transparency for the probe field [see Fig. 2(a)], then more light is transmitted the medium. The other is due to the SGC enhanced nonlinear absorption [see Fig. 2(c)], which increases the absorption modulation depth. As a result, more light can be diffracted into the first order diffraction component which located at $\sin\theta = \lambda_p / \Lambda = 0.25$. Using Eq. (7b) which taking only third order susceptibilities into account, we plot respectively the amplitude, phase and diffraction patterns in Figs. 4(a), 4(b) and 4(c) with green dash-dot line. As can be seen, it is the SGC enhanced third order nonlinearity with vanishing linear absorption that contributes mainly to the absorption modulation and the diffraction patterns.

The diffraction efficiency, which is determined by the nonlinear absorption modulation, depends strongly on the intensity of trigger field Ω_T and the interaction length L. Figure 5 illustrates how these parameters affect the first order diffraction efficiency. Figure 5(a) shows the first order diffraction intensity as a function of Ω_{T0}. As the intensity of trigger field increases, the nonlinear absorption modulation depth increases, thus improving the diffraction power of the grating. However, it peaks at certain Ω_{T0}, beyond which it fades away due to the decrease of average transmissivity as a result of increased nonlinear absorption. The result is the same when the interaction length L varies, as shown in Fig. 5(b).

B. Phase grating

The diffraction efficiency attainable by the pure absorption grating is limited (6.25% for an ideal sinusoidal absorption grating and 4% in our above results). The fact is that the absorption modulation tends to gather light to the center maximal (zero order diffraction) and the light absorption is dominant. In order to increase the diffraction efficiency, we wish the medium that is transparent to the probe, but can induce a π phase modulation across the probe field. Fortunately, the SGC induced transparency and enhanced nonlinear refraction with off resonant trigger field meet such conditions, hence a phase grating can be formed with the help of SGC. The numerical results are illustrated in figure 6. In the case of without SGC, although the phase modulation is large enough [about 0.65π with red dashed line in Fig. (6b)], the probe field is almost completely absorbed [red dashed line in Fig. (6a)], hence the first order diffraction efficiency is extremely low [$0.6\times10^{-54}\%$ in Fig. (6d)]. While SGC is present, we can obtain a phase modulation on the order of π [black solid line in Fig. (6b)] with small nonlinear absorption modulation which oscillates around an average transmissivity of 95% [black solid line in Fig. (6a)]. The phase modulation diffracts a significant portion of the probe energy into two first-order patterns ($\sin\theta = \pm 0.25$) and a small portion into the two second diffraction order ($\sin\theta = \pm 0.5$). The resulting first order diffraction efficiency of the grating is 31% which is very close to that of an ideal sinusoidal phase grating (about 34%).

The role of SGC in the formation of phase grating is to enhance Kerr nonlinearity and restrain absorption, and then almost pure phase modulation can be achieved. In Figs. 6(a), 6(b) and 6(c), we plot respectively the amplitude, phase and diffraction patterns induced by the third order nonlinear susceptibility with green dash-dot line. It is clear that the π phase modulation and the efficient diffraction are mainly due to the enhanced Kerr nonlinearity with neglectable

absorption induced by the SGC effect.

Figure 7 displays the first order diffraction intensity as a function of the trigger field Ω_{T0} and the interaction length L. It shows that an optimum value of Ω_{T0} or L exists for which the energy of light in the first order is significant increased. For large Ω_{T0} or L, the nonlinear absorption is dominant, then the diffraction efficiency decreases.

IV. CONCLUTION

We have investigated the effect of SGC on the third order nonlinearity in a ladder-type atomic system. It is found that SGC is capable of enhancing the nonlinearity. With a resonant trigger field, two-photon absorption is enhanced by the constructive quantum interference while maintaining linear absorption vanishing due to the SGC effect. However, with large off resonant trigger field, a large nonlinear refraction can be obtained accompanied by neglectable nonlinear absorption. Such SGC assisted enhancement of nonlinear absorption or refraction allow us to achieve efficient pure absorption or phase grating when the trigger has a standing-wave pattern. In the formation of electromagnetically induced grating, the role of SGC is twofold. The SGC effect can make the opaque medium transparent via destructive interference, then the transmissivity for the probe is greatly increased and more light is available to be diffracted. Furthermore, SGC can enhance the absorption or phase modulation depth, and therefore, the diffraction power of the grating is increased. The all optically induced gratings may have applications in light switching and routing. It is worth noting here that the enhancement of nonlinearity in this system is a result of inherent quantum interference in the decay so that no coupling laser fields are required for creating transparency. Moreover, the present gratings arise from the nonlinear modulation which is different from the recent EIG schemes based on linear modulation. Finally, it should be emphasized that, although the existence of SGC needs for

nonorthogonal dipole moments and near-degenerate close-lying upper levels which are rarely met in real atoms and become the bottleneck in the observation of the predicted new effects [32], such type of quantum interference can be observed in many incoherent decay processes. Example include spontaneous emission in molecules [33], autoionizing resonances [34, 35], and tunneling effect in quantum wells [36-38]. When the atom couples to cavity field or anisotropy vacuum, quantum interference occurs even if the corresponding dipole moments are orthogonal [39-41]. Moreover, the SGC effect can also be simulated in the dressed atoms interacting with dc field, laser field or microwave field [42-45]. Therefore, our proposed scheme can be equally applied to the above systems where such interference exists.

ACKNOLEDGEMENTS

This work is supported by NSFC (Grant No. 10774059, 11074097), and the National Basic Research Program (Grant No. 2006CB921103, 2011CB921603) of the People's Republic of China.

REFRENCES

[1] C. Ottaviani, D. Vitali, M. Artoni, F. Cataliotti, and P. Tombesi, Phys. Rev. Lett. **90**, 197902 (2003).

[2] S. Rebic, D. Vitali, C. Ottaviani, P. Tombesi, M. Artoni, F. Cataliotti, and R. Corbalán, Phys. Rev. A **70**, 032317 (2004).

[3] A. Joshi, and M. Xiao, Phys. Rev. A **72**, 062319 (2005).

[4] S. E. Harris, and Y. Yamamoto, Phys. Rev. Lett. **81**, 3611 (1998).

[5] M. Yan, E. G. Rickey, and Y. F. Zhu, Phys. Rev. A **64**, 041801 (2001).

[6] Y. Wu, and L. Deng, Phys. Rev. Lett. **93**, 143904 (2004).

[7] G. X. Huang, C. Hang, and L. Deng, Phys. Rev. A **77**, 011803 (2008).

[8] H. Schmidt, and A. Imamoğlu, Opt. Lett. **21**, 1936 (1996).

[9] H. Kang, and Y. F. Zhu, Phys. Rev. Lett. **91**, 093601 (2003).

[10] Y. F. Chen, C. Y. Wang, S. H. Wang, and I. A. Yu, Phys. Rev. Lett. **96**, 043603 (2006).

[11] S. J. Li, X. D. Yang, X. M. Cao, C. H. Zhang, C. D. Xie, and H. Wang, Phys. Rev. Lett. **101**, 073602 (2008).

[12] H. Wang, D. Goorskey, and M. Xiao, Phys. Rev. Lett. **87**, 073601 (2001).

[13] Y. P. Niu, S. Q. Gong, R. X. Li, Z. Z. Xu, and X. Y. Liang, Opt. Lett. **24**, 3371 (2005).

[14] L. Deng, M. G. Payne, Phys. Rev. Lett. **98**, 253902 (2007).

[15] S. E. Harris, Phys. Rev. Lett. **62**, 1033 (1989).

[16] J. H. Wu, and J. Y. Gao, Phys. Rev. A. **65**, 063807 (2002).

[17] G. S. Agarwal, *Quamtum Optics*, Springer Tracks in Modern Physics Vol 70 (Spriger-Verlag, Berlin, 1974).

[18] S. Y. Zhu, R. C. F. Chan, C. P. Lee, Phys. Rev. A **52**, 710 (1995).

[19] S. Y. Zhu, and M. O. Scully, Phys. Rev. Lett. **76**, 388 (1996).

[20] P. Zhou, and S. Swain, Phys. Rev. Lett. **77**, 3995 (1996).

[21] E. Paspalakis, and P. L. Knight, Phys. Rev. Lett. **81**, 293 (1998).

[22] K. T. Kapale, M. O. Scully, S. Y. Zhu, and M. S. Zubairy, Phys. Rev. A **67**, 023804 (2003).

[23] V. V. Kozlov, Y. Rostovtsev, and M. O. Scully, Phys. Rev. A **74**, 063829 (2006).

[24] W. H. Xu, J. H. Wu, and J. Y. Gao, Eur. Phys. J. D **30**, 137 (2004).

[25] Y. P. Niu, and S. Q. Gong, Phys. Rev. A **73**, 053811 (2006).

[26] P. Zhou, and S Swain, Phys. Rev. Lett. **78**, 832 (1997).

[27] E. Paspalakis, N. J. Kylstra, and P. L. Knight, Phys. Rev. Lett. **82**, 2079 (1999).

[28] H. Y. Ling, Y. Q. Li, and M. Xiao, Phys. Rev. A **57**, 1338 (1998).

[29] B. K. Dutta, and P. K. Mahapatra, J. Phys. B **39**, 1145 (2006).

[30] Z. H. Xiao, S. G. Shin, and K. Kim, J. Phys. B **43**, 161004 (2010).

[31] L. E. E. de Araujo, Opt. Lett. **35**, 977 (2010).

[32] A. Imamoğlu, Phys. Rev. A **40**, 2835 (1989).

[33] H. R. Xia, C. Y. Ye, and S. Y. Zhu, Phys. Rev. Lett. **77**, 1032 (1996).

[34] K. H. Hahn, D. A. King, and S. E. Harris, Phys. Rev. Lett. **65**, 2777 (1990).

[35] T. Nakajima, Opt. Lett. **25**, 847 (2000).

[36] J. Faist, F. Capasso, C. Sirtori, K. W. West, and L. N. Pfeiffer, Nature (London) **390**, 589 (1997).

[37] H. Schmidt, K. L. Campman, A. C. Gossard, and A. Imamoğlu, Appl. Phys. Lett. **70**, 3455 (1997).

[38] J. H. Wu, J. Y. Gao, J. H.. Xu, L. Silvestri, M. Artoni, G. C. La Rocca, and F. Bassani, Phys. Rev. Lett. **95**, 057401 (2005).

[39] A. K. Patnaik, and G. S. Agarwal, Phys. Rev. A **59**, 3015 (1999).

[40] P. Zhou, and S. Swaim, Opt. Commun. **179**, 267 (2000).

[41] G. S. Agarwal, Phys. Rev. Lett. **84**, 5500 (2000).

[42] K. Hakuta, L. Marmet, and B. P. Stoicheff, Phys. Rev. Lett. **66**, 596 (1991).

[43] Z. Ficek, and S. Swain, Phys. Rev. A **69**, 023401 (2004).

[44] J. H. Wu, A. J. Li, Y. Ding, Y. C. Zhao, and J.Y. Gao, Phys. Rev. A **72**, 023802 (2005).

[45] A. J. Li, X. L. Song, X. G. Wei, L. Wang, and J. Y. Gao, Phys. Rev. A **77**, 053806 (2008).

Figure captions

FIG. 1. (Color online) (a) Schematic diagram of a four-level double Ladder-type system with two closely spaced upper levels $|2\rangle$ and $|3\rangle$ strongly coupled via spontaneous emission. A trigger field E_T couples levels $|2\rangle$ and $|3\rangle$ to an exited level $|4\rangle$, while a weak probe field E_p interacts with $|1\rangle \leftrightarrow |2\rangle$ and $|1\rangle \leftrightarrow |3\rangle$ transitions. (b) Arrangement of the probe (trigger) electric field $\vec{E}_p$ ($\vec{E}_T$) and the relevant dipole moments $\vec{d}_{12}$ and $\vec{d}_{13}$ ($\vec{d}_{24}$ and $\vec{d}_{34}$).

FIG. 2. (Color online) Evolutions of absorptive and refractive parts of $\chi^{(1)}$ and $\chi^{(3)}$ versus the probe detuning Δ_p in the cases of with (black solid curve) and without (red dashed curve) SGC. Parameters are $\Gamma_2 = \Gamma_3 = \Gamma_4 = \gamma$, $\delta = \gamma$, $\Delta_T = 0$ in (c) and (d), $\Delta_T = -25\gamma$ in (e) and (f).

FIG. 3. Sketch of the spatial configuration of the probe and trigger field.

FIG. 4. (Color online) (a) The absorption modulation for the probe. (b) The phase modulation for the probe. (c) The diffraction pattern as a function of $\sin(\theta)$ with SGC. (d) The diffraction pattern as a function of $\sin(\theta)$ without SGC. The black solid and red dashed curves correspond to the cases with and without SGC when considering all orders susceptibilities. The green dash-dot curves display the case of only taking the third order nonlinearity into account. Parameters are as follows: $\Omega_{T0} = 0.5\gamma$, Λ=4, $M = 5$, $L = 2z_0$. Other parameters are the same as in Fig. 2 (c) and 2(d).

FIG. 5. The first order diffraction intensity $I_p(\theta_1)$ as a function of Ω_{T0} (a) and L (b), respectively. The parameters are the same as in Fig. 4.

FIG. 6. (Color online) (a) The absorption modulation for the probe. (b) The phase modulation for the probe. (c) The diffraction pattern as a function of $\sin(\theta)$ with SGC. (d) The diffraction pattern as a function of $\sin(\theta)$ without SGC. The black solid and red dashed curves correspond to the cases with and without SGC when considering all orders susceptibilities. The green dash-dot curves display the case of only taking the third order nonlinearity into account. Parameters are as follows: $\Omega_{T0} = 0.5\gamma$, Λ=4, $M = 5$, $L = 80z_0$. Other parameters are the same as in Fig. 2 (e) and 2(f).

FIG. 7. The first order diffraction intensity $I_p(\theta_1)$ as a function of Ω_{T0} (a) and L (b), respectively. The parameters are the same as in Fig. 6.

Figures

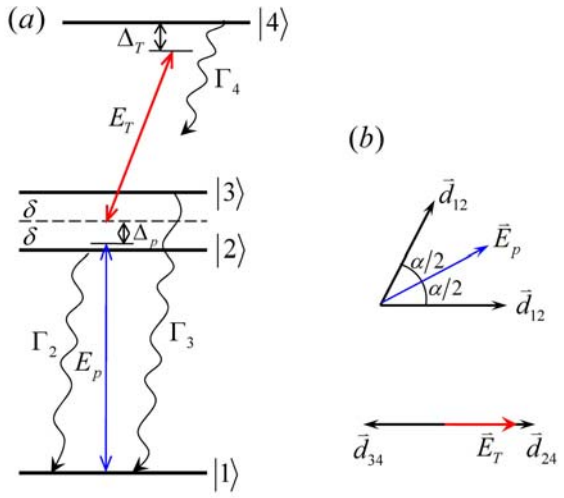

FIG. 1

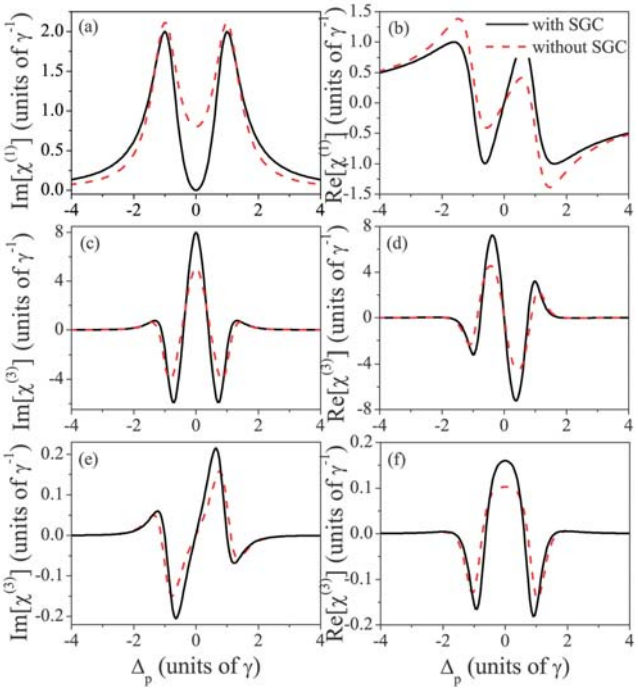

FIG. 2

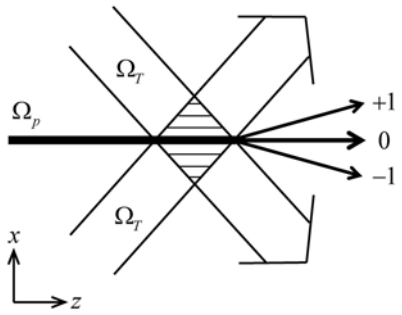

FIG. 3

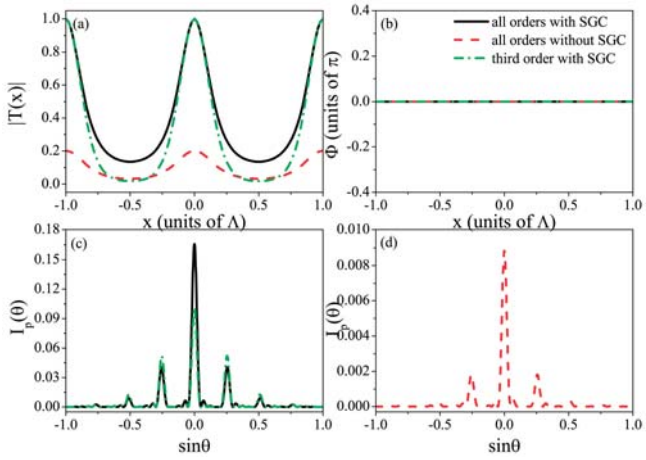

FIG. 4

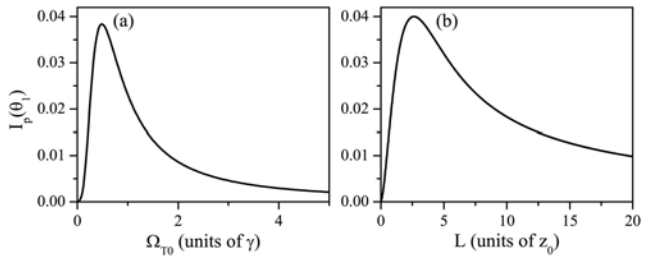

FIG. 5

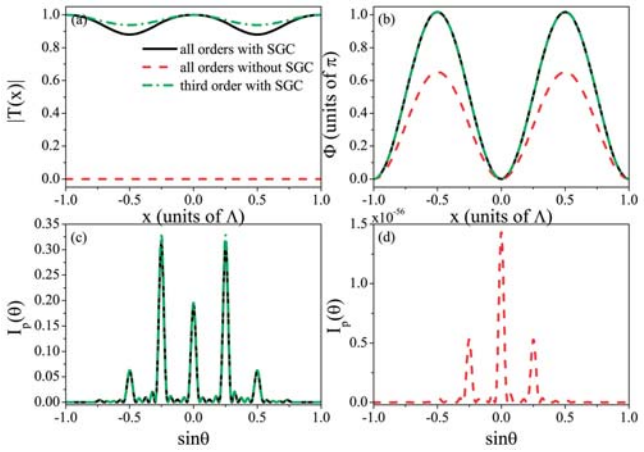
(a)
all orders with SGC
all orders without SGC
third order with SGC
|T(x)|
x (units of Λ)
(b)
Φ (units of π)
x (units of Λ)
(c)
I_p(θ)
sinθ
(d)
x10^-56
I_p(θ)
sinθ

FIG. 6

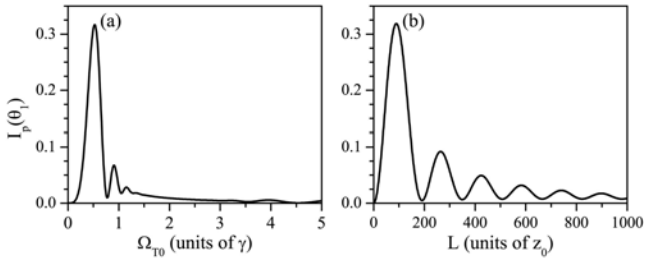
(a)
I_p(θ_1)
Ω_T0 (units of γ)
(b)
L (units of z_0)

FIG. 7